UNCLASSIFIED

DEPARTMENT OF DEFENCE

DSTO

Land, Space and Optoelectronics Division

RESEARCH REPORT
SRL-0117-RR

ADVANCED INFRARED PHOTODETECTORS
(MATERIALS REVIEW)

by

Philip J. Picone

SURVEILLANCE RESEARCH LABORATORY

APPROVED FOR PUBLIC RELEASE

UNCLASSIFIED

AR-008-157

DSTO AUSTRALIA

SURVEILLANCE RESEARCH LABORATORY

Land, Space and Optoelectronics Division

RESEARCH REPORT
SRL-0117-RR

ADVANCED INFRARED PHOTODETECTORS (MATERIALS REVIEW)

by

Philip J. Picone

SUMMARY

The present status of advanced infrared semiconductor detector materials and their application to infrared sensor array systems is reviewed. Techniques to increase device operating temperature are considered for various materials. Focal plane processing requirements are also considered.

DECEMBER 93 COPY No.

APPROVED FOR PUBLIC RELEASE

POSTAL ADDRESS: Director, Surveillance Research Laboratory, PO Box 1500, Salisbury, South Australia, 5108.

CONTENTS

FIGURES

TABLES

ABBREVIATIONS

ATDR	Automatic Target Detection/Recognition
BLIP	Background Limited Infrared Photodetector
CMT	Cadmium Mercury Telluride
DMS	Dilute Magnetic Semiconductor
FOV	Field of View
FPP	Focal Plane Processing
IR	Infrared
LPE	Liquid Phase Epitaxy
LWIR	Long Wave Infrared (8 - 12 μm)
MBE	Molecular Beam Epitaxy
MCMT	Mercury Cadmium Manganese Telluride
mm-WAVE	Millimetre wave
MMT	Mercury Manganese Telluride
MQW	Multiple Quantum Well
MWIR	Medium Wave Infrared (3 - 5 μm)
MZT	Mercury Zinc Telluride
NEP	Noise Equivalent Power
NEΔT (NETD)	Noise Equivalent Temperature Difference
NUC	Non-Uniformity Correction
PC	Photoconductor
PV	Photovoltaic
SLS	Strain Layer Superlattice
SPRITE	Signal PRocessing In The Element
SWIR	Short Wave Infrared (1 - 3 μm)
TDI	Time Delay Integration
UV	Ultraviolet
VLSI	Very Large Scale Integrated
VLWIR	Very Long Wave Infrared (14 - 30 μm)
VPE	Vapour Phase Epitaxy

THIS IS A BLANK PAGE

1. INTRODUCTION

The purpose of this review is to examine the current status of advanced infrared (IR) detector materials. An overview of the requirements of the detector material and focal plane processing is followed by a discussion on the present status of advanced IR semiconductor materials and their application to photodetectors.

Infrared detectors can be separated into two classes. The first type can be classified as a "thermal" detector where a material property (eg resistance) varies with the temperature of the detecting element. These devices effectively operate in two "steps" where:

(1) the detector material absorbs infrared energy causing a temperature increase, and

(2) the resultant temperature change is measured as a temperature dependent material property.

The infrared signal is measured through the variation in the material property. This two "step" operation has disadvantages, notably in response time and sensitivity. Its main advantages are its broad spectral coverage and possible room temperature operation.

This is in contrast to the second type of infrared detector that utilises "photon" or photosensitive materials. "Photon" detection refers to materials that generate electron/hole pairs from the direct absorption of infrared radiation. This generated photo current or photo voltage is used as the infrared signal measurement. The advantages include a fast response time and high sensitivity, but it has the disadvantage that room temperature operation is difficult due to high thermal noise levels.

Direct detection of photons requires the energy gap of the material to be less than the photon energy. For infrared wavelengths the photon energies are, for example, 0.25 eV at 5 μm and 0.1 eV at 12 μm. Because thermal energy, kT, at room temperature is approximately 0.025 eV, a significant fraction of the energy gap required for IR detection, "photon" detectors need to be operated at low temperatures in order to minimise thermal noise. The narrow energy gap is either a characteristic of the semiconductor material or generated in multilayer devices. Two types of multilayer structures are used, these being strained layer superlattices where the energy bands are altered by the effects of strain, or multiple quantum wells where the energy bands are engineered, both to allow absorption at the required wavelength.

In the rest of this report it is intended to concentrate mainly on photosensitive materials. A number of reviews on the current status of bolometer detectors are available [56,57]. For many applications, bolometer detectors meet the system requirements and should not be discounted. In addition, the section on focal plane processing in this report can apply to bolometer detectors as well as photosensitive detectors.

The probable requirements for infrared image detection in the future can be summarised as follows:

(a) large format staring arrays (10^4 - 10^6 elements) operating at TV frame rates.

(b) large linear arrays (480 x 4 and up to 4096 x 4 elements) for wide field of view.

(c) multi-spectral (3-5, 8-12 μm) and multi band (UV - IR, IR - mm-wave) operation to increase detection probability, reduce false alarm rates and perform automatic target detection/recognition (ATDR),

(d) focal plane processing for real time image analysis/identification,

(e) near room temperature operation,

The detector material in this generation of IR system [1,2,3] is the critical factor linking detector array, IR detection system and manufacture as shown in Figure 1. As a prerequisite, high quality semiconductor material will be required for the detector array. Sensitivity, spectral band, noise spectrum, spatial uniformity, input power and reliability are system parameters with a direct relationship to the IR material. As a consequence the manufacturer of the detector module will need considerable expertise in semiconductor processing; firstly to make the detector array, secondly to enable data manipulation in the focal plane and finally to output the results to the display electronics. For example, in the hybrid technologies the detector material and the readout electronics are generally different semiconductors and the two have to be bonded together, thus introducing material compatibility complications.

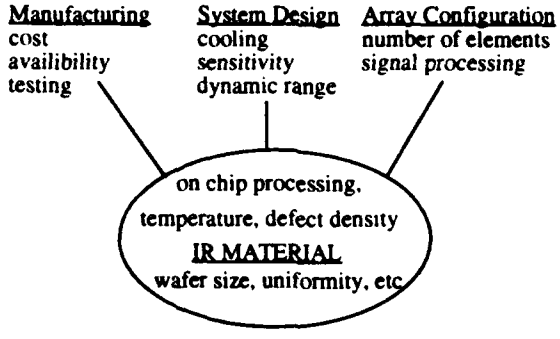

Figure 1 Infrared material and links to the IR system

Operating temperature and spatial response uniformity are two of the most important parameters in detector systems. These two areas will be discussed in general followed by a short discussion on focal plane processing.

2. INFRARED DETECTOR OPERATION AND PERFORMANCE.

2.1 Noise considerations.

Before discussing the operating temperature or spatial uniformity of IR systems, the basic limitations on detection needs to be considered. Ultimately the performance of an IR sensor is limited by variations in the photon background statistics, manifested as a variation in the generation/recombination (GR) rate, and more commonly referred to as Background Limited Infrared Photodetector (BLIP) performance. Other noise sources, for example internal GR, Auger sources and 1/f noise, are sensor dependent and can be minimised by reducing unintentional dopants in the semiconductor (impurities or vacancies) or by

reducing the sensor operating temperature. A commonly used figure of merit for an IR sensor material is the detectivity (D^*) which reflects the measured signal to noise ratio under specified conditions of IR flux and field of view. D^* is normalised with respect to bandwidth and detector area, being defined as:

$$D^* = (A\Delta f)^{1/2} / NEP \qquad (1)$$

where A is the detector area, Δf the bandwidth and NEP the noise equivalent power. The NEP is defined as the required level of power, within a specified spectral band, incident on the detector to obtain a photon signal level equal to the electronic noise level. For a photodiode detector, and ignoring 1/f noise, equation 1 can be written as [2,58];

$$D^* = \eta\left(\eta\Phi_B + 2kT / q^2 R_o A + g_{th} d\right)^{-0.5} / \sqrt{2} E_\lambda \qquad (2)$$

where η is the quantum efficiency, E_λ the energy at wavelength λ, Φ_B is the background photon flux, k is Boltzmans constant, T is the device temperature, q the electronic charge, g_{th} is the electron-hole photogeneration rate density and d is the photodetector thickness. R_0 is defined as the zero bias impedance of the diode. The first term is photon background noise and the second the Johnson noise. Typically measured D^* values for the 3-5 and 8-12 μm spectral bands with ambient temperature backgrounds are on the order 10^{11} cm $Hz^{1/2}W^{-1}$ and 10^{10} cm $Hz^{1/2}W^{-1}$ respectively.

For an ideal detector with no Johnson and thermal generation noise, the detectivity is limited by the photon background and is given by;

$$D^*_{BLIP} = (\eta / \Phi_B)^{0.5} / \sqrt{2} E_\lambda \qquad (3)$$

BLIP performance implies that the device noise sources can be reduced below the photon noise level (equation 3). In some applications this places extremely low limits on the internal noise level which, as a consequence, requires junction and material properties at or beyond current state-of-art. For a photodiode the noise sources can be dominated by Johnson noise; that is, the photogeneration and photon background noise can be neglected by comparison. In this situation the detectivity can be approximated by:

$$D^*_J = \eta q (R_o A / kT)^{0.5} / 2E_\lambda \qquad (4)$$

In the Johnson noise limit for a photodiode (equation 4) the detectivity is proportional to $(R_oA)^{0.5}$. For hybrid focal plane arrays this must be large, not only for sensitivity, but also for coupling to readout circuits. For cadmium mercury telluride (CMT) R_oA is approximately 10^5 Ωcm^2 for 3-5 μm and 10 Ω cm^2 for 8-12 μm operation [2].

2.2 Operating Temperature.

As stated earlier, the semiconductor band gap has to be smaller to allow detectors to function at longer wavelengths, and is almost the same order of magnitude as the thermal energy kT at room temperature.

In Table 1 the semiconductor cutoff wavelength is presented as a function of temperature for a number of materials. In part, this table shows that for long wavelength operation low temperatures are required as expected. The cutoff wavelength for any particular material also shifts as the energy gap varies with temperature. The operating wavelengths of strained layer superlattices and multiple quantum wells vary depending upon the structure but require low operating temperatures.

Table 1. Detector cutoff wavelength for various materials

Detector	Wavelength Limit (μm)			
Temperature K	300K	190K	80K	1.5 -60K
PbS	3.0	3.3	3.6	-
PbSe	4.4	5.4	6.5	-
InSb	7.0	6.1	5.5	5.0
PtSi	-	-	4.8	10 - 16
PV CdHgTe	1 - 3	1 - 5	3 - 12	12 - 25
PC CdHgTe	1 - 11	3 - 11	5 - 25	-
GaAs/GaAlAs type MQW	-	-	-	9
InAs/InAsSb type SLS	-	-	-	8 - 14
InP/InAsP type MQW	-	-	7 - 12	-

The need for cooling depends on the material and the operating wavelength. In general, to operate at temperatures where thermal noise is not a problem, temperatures less than 80K are required for detectors in the Long Wave (8-14μm) IR and in the Very Long Wavelength (14-30μm) region. In the Medium IR (3-5μm), operation up to 190K is possible with some materials. At Short Wave IR, room temperature operation is normal. Photoconductive (PC) cadmium mercury telluride ($Cd_xHg_{1-x}Te$, x ~ 0.167) has a LWIR cutoff at room temperature; however, operation is typically at low temperatures to reduce thermal noise. Further, this type of detector is not amenable to large array fabrication due to power dissipation problems (all of the individual detectors need to be biased) and the difficulty of interfacing to read-out structures. Because of these problems, photovoltaic (PV) material is generally used for large staring arrays.

2.3 Techniques to increase the operating temperature.

A number of techniques have been used in attempts to raise the operating temperature of two dimensional arrays and thereby to reduce the requirement for large power-consuming cooling devices. The main two which have the most promise for 2D arrays are discussed below.

2.3.1 Micro lens arrays (optical immersion).

With IR detector arrays the diode junction cannot occupy all of the available space on the chip surface. Diodes need to be isolated from each other and some area may be required for signal processing. Because of these factors the detector fill factor can be as low as 10%. This results in

a loss of IR signal. By using lenses to focus the IR radiation onto the junction this signal can be recovered. Secondly, the R_oA product of the diode is increased through the effective increase in junction area. This leads to an increase in the detectivity (equation 4) for the detector.

The lens arrays are micro fabricated in silicon, gallium arsenide (GaAs) or cadmium telluride (CdTe) at the same spacing as the detector elements [5,6,7,8,59]. They are bonded to the detector array and serve to increase the effective detector area (Figure 2). Lens plates have been made by two processes. In the first, a photoresist layer is etched and thermally shaped into lenses protruding from the substrate. This shape is then transferred by controlled milling. In the second technique, photoresist masks and etching are used to form a lens with a series of steps etched directly onto the substrate. Unless these processes are accurate, only limited gains will be achieved. Lens aberration will defocus the beam and reduce the power incident on the detecting element, defeating the purpose of the microlens.

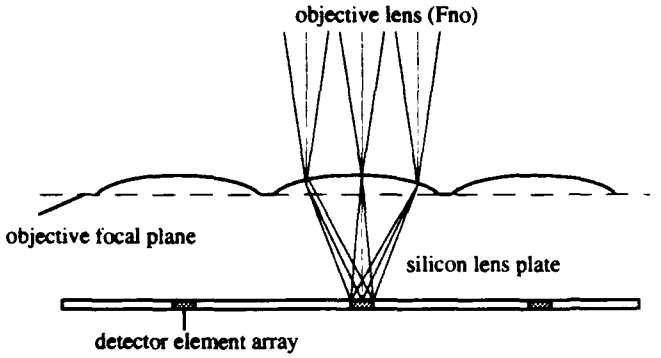

Figure 2. Microlens array.

Considering a square microlens (side p, refractive index n and Fno of the objective lens) concentrating the incident radiation onto a square detector (side s), the area gain is:

$$\text{area gain} = p^2/s^2 = \left(p(n-1)Fn_o\right)^2 \qquad (5)$$

The maximum gain is limited due to total internal reflection at the lens/detector interface as governed by the refractive index of the glue [6,8] used to bond the lens plate to the detector array. In this case the area gain is given by:

$$\text{area gain (glue limited)} = \left(2n_{glue}Fn_o\right)^2 \qquad (6)$$

If the refractive index of the glue is 1.5, the area gain is limited to 17 for an *f*/4 system. Results for an optically immersed CMT array [8] with photocurrent gains of around 10-12 are less than expected and further work is required to approach the theoretically expected gain. Epitaxially grown lenses, or lenses fabricated in the detector substrate, will overcome the lens/glue/detector interface limitations. In this case, maximum gains of up to 100 may be possible [6]. For a CMT MWIR array a gain of 50 would lead to an increase in D^* of approximately 7 (equation 1) or alternatively to an increase in the operating temperature from 150K to 245K for equivalent noise

performance. A microlens fabricated in CdTe with an epitaxially deposited CMT detector [59] gave approximate photocurrent gains of 2-3 at 30°K. This is less than expected with alignment errors, lens fabrication irregularities, no IR coating and the low operating temperature all contributing to the lower gain. A further feature of using a microlens is to provide some protection to the IR array from γ-rays by reducing the effective detector area [9]. The lens structure also offers a measure of mechanical protection.

2.3.2 Electronic non-equilibrium techniques.

A number of electronic material techniques [10,63], as distinct from signal processing techniques, have been investigated to reduce device noise to BLIP level by reducing the noise (Auger, internal generation / recombination) sources. It is then possible to raise the operating temperature until the noise floor begins to limit the device operation. In general, high quality material is required to implement these techniques.

(1) Multi layer structures.

In the first technique a multilayer structure with different dopants is formed in the IR semiconductor [10] (Figure 3), the effect of which is to reduce the electron and hole concentrations from their intrinsic values to levels typical of extrinsic conditions. This achieves two results: firstly, conduction processes in the devices are controlled by the dopants and secondly, the leakage currents and consequent noise are reduced by suppression of the dominant Auger generation mechanisms. The device is then a minority carrier extraction diode based on near intrinsic p-type material. The technique does require the semiconductor to be very pure and defect free so that excess carriers do not dominate the noise process. The junctions formed in the semiconductor may be either $p^+\pi n^+$ or $\underline{p}\pi\underline{n}$ where :

p^+, n^+ are heavily doped p or n layers,
π is p type doped to near intrinsic, and
$\underline{p}$, $\underline{n}$ are wide gap p, n material respectively.

The technique is applicable to narrow gap semiconductors and can be implemented with Molecular Beam Epitaxy (MBE). The principal of operation is to reduce the number of free carriers in the π (detection) region to very low levels. This has the effect of reducing the noise sources. At temperatures where the π region is near intrinsic and under reverse bias, minority carrier extraction occurs at the $\pi\, n^+$ ($\pi\, \underline{n}$) diode junction resulting in a large reduction in carrier density in its vicinity. The p^+ (p) material forms an excluding contact to the π material preventing the injection of electrons to replace those removed at the diode junction.

A four layer device[10] ($p^+\underline{p}\pi n^+$) has also been constructed in $InSb/In_{1-x}Al_xSb$. A thin $\underline{p}$ layer, typically 0.02 μm, forms a potential barrier and further reduces tunnelling from the p^+ region. Because of this, the electron density drops by several orders of magnitude throughout the π

region. The hole concentration must do likewise, to maintain charge neutrality and to consequently reduce noise sources. $InSb/In_{1-x}Al_xSb$ multilayer diodes grown by MBE have been shown to have the same performance at room temperature as conventional diodes that are cooled cryogenically.

Current state-of-art CMT materials technology, - namely, MBE, Liquid Phase Epitaxy (LPE), Vapour Phase Epitaxy (VPE) and bulk growth - has not advanced sufficiently to reduce the high intrinsic conduction levels sufficiently to allow the construction of the two terminal (three layer Figure 3(a)) or four layer Figure (3(b)) devices. However, a three terminal device Figure (3(c)) has been fabricated in CMT [10]. The extra diode junction formed acts as a sink for electrons, reductions in leakage currents through the detector junction of up to 50 having been observed.

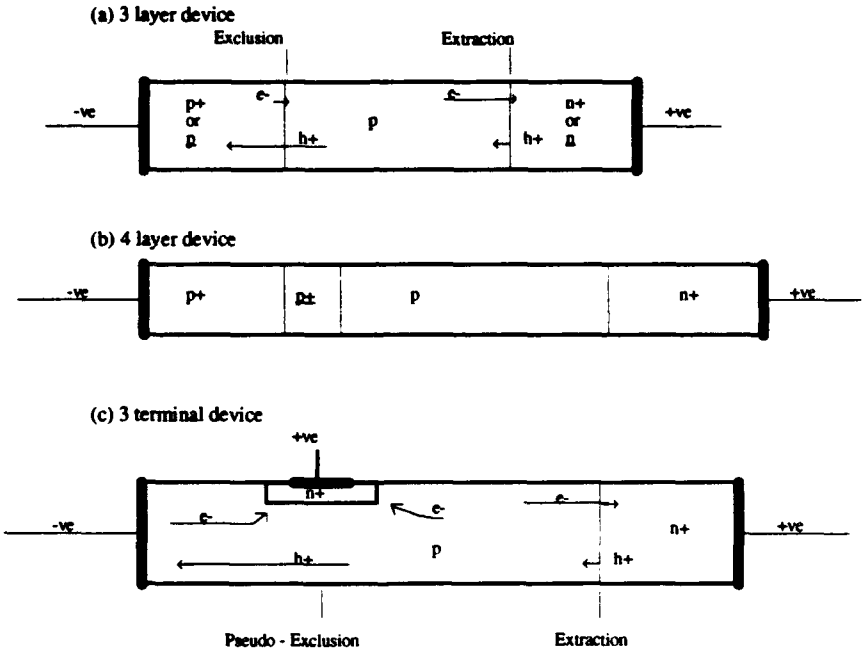

Figure 3. Schematic non-equilibrium diode structures showing (a) two-terminal exclusion-extraction (3 layer device), (b) 4 layer device and (c) three-terminal proximity extraction devices.

(2) Time Delay Integration and SPRITE detectors

Time Delay Integration (TDI) and Signal PRocessing In The Element (SPRITE) are two electronic means for integrating the IR signal in the detector element and thereby improving the signal to noise ratio. TDI works by summing adjacent elements in an array (eg 128 x 4) as the IR signal is scanned across the 4 elements. The signal from adjacent elements across the array is delayed by the scan time between elements (Figure 4). This results in an output signal larger than obtained from a single detecting element. resulting in improved signal to noise ratio.

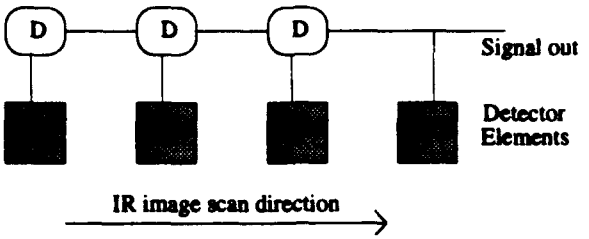

Figure 4. Schematic TDI scan geometry. D is the Dwell time.

SPRITE detectors were developed to perform the integration in the detector element and not externally as in TDI. A long thin element is used and the IR signal is integrated as it scans the length of the element (Figure 5). In SPRITE elements the scan rate is set equal to the carrier drift rate.

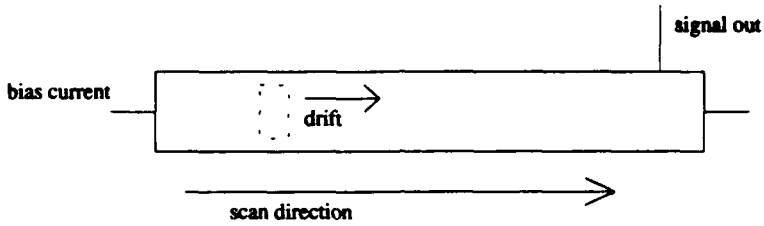

Figure 5. Schematic SPRITE element. The carrier drift rate equals the image scan rate.

Both techniques are only possible in linear arrays and cannot realistically be implemented in 2D staring arrays. Further, for the SPRITE configuration, (which is only applicable in photoconductive detectors), the microlens technique is difficult to implement.

(3) Magneto concentration

This technique is based on the magneto concentration effect [11]. A magnetic field is applied normal to the electric field (bias field), the action of the Lorentz force causing the transport of holes and electrons to the backside of the detector thereby resulting in a depletion across most of the semiconductor (Figure 6). Theoretical calculations show a marked increase in the normalised detectivity, leading to higher temperature operation. An added complication is the application of a magnetic field to the detector. Again this is only applicable to photoconductors. This structure has been implemented in an InSb PC detector [62] and resulted in a photoresponse gain of approximately 10 for an electric field (E) of 30 V/cm and magnetic field (B) of 1.5 Tesla.

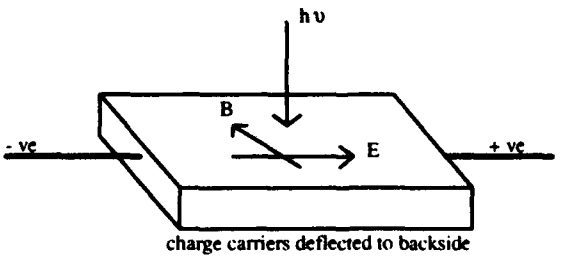

Figure 6. Schematic diagram of magneto concentration detector.

In summary, the combination of the electronic non-equilibrium noise reduction techniques and gains made by optical immersion (microlens) appears promising for the production of detectors that will operate at higher temperatures. Near BLIP performance is expected to be achieved at 250K for 3-5 μm InSb detectors thus enabling simple thermoelectric cooling. Higher temperature operation in CMT is more uncertain as material problems make electronic non-equilibrium noise reduction techniques difficult. The techniques do, however, still require extensive materials development and processing advances. For 8-12 μm CMT detectors, it is expected that low temperatures, (< 200K [8]), will still be required due to the higher intrinsic thermally generated noise.

3. FOCAL PLANE PROCESSING

Focal plane processing (FPP) is a new and developing area for IR detectors and is expected to be an important component in the next generation of IR sensor systems. Table 2 indicates some of the applications leading to on-chip signal processing requirements. The sensor processing requirement is related to the generic application. For example, information from multi-spectral arrays will be needed to improve the detection probability, reduce the false alarm rate and to discriminate the target from the background or other targets/decoys. On chip image processing will enable optimised information processing and possible autonomous operation.

Table 2. Applications and Requirements for focal plane processing.

Generic Application	Sensor Processing Requirement
Long-range surveillance	Multiple high density arrays with individual sensor selection
Autonomous recognition	On-chip image processing
Target discrimination	Multi-spectral processing
Real-time decision-making	High speed readout
Variable background operation	Adaptive signal conditioning at the detector
High reliability, lightweight	On-chip clocks and bias circuits

An initial use of FPP is nonuniformity correction (NUC) since spatial response nonuniformity is one of the crucial limiting factors in detector arrays. Nonuniformity correction leads to signal processing overhead, to increased power consumption and a reduction of the sensor's dynamic range. Residual nonuniformity ultimately limits the signal to noise ratio of the imaging system. For example, in high flux conditions the nonuniformity dominates the signal to noise ratio to such an extent that a detector characterised by a low quantum efficiency but high pixel uniformity (1%, 0.1% respectively) will out-perform a system with high quantum efficiency but poor uniformity (100%, 1%) [4]. In low flux conditions the quantum efficiency limits the sensor performance. With more uniform material, the processing capability no longer required for NUC could be used for image processing.

Device geometry precision requirements can also contribute to pixel-to-pixel nonuniformity. A critical dimension can be defined from the combined errors arising from the mask alignment inaccuracies.

photoresist exposure and development, device etching and other processes which lead to device geometry variations [4]. For example, for a detector optical area of 10^{-4} cm^2 (0.01 cm sq pixel) characterised by a critical dimension of 1 μm, the uniformity is limited to at best ~ 2%. At present, PtSi detectors appear to be limited by photolithography accuracy, PV CMT is limited by device geometry while InSb detectors fall somewhere between these two [4]. Self alignment techniques are improving this accuracy. CMT also has material problems such as composition inhomogeneity which lead to large variations in response which can swamp the geometry variations.

Standard NUC techniques involve calibrating each pixel with gain and offset adjustments using a reference temperature source. Usually the correction factors need to be re-calibrated after a short period of time due to system drift or changes in the background level. Focal plane processors can be programmed to correct for pixel variations: however, adaptive [12] techniques have been proposed when recalibration is a problem. Adaptive techniques that have been considered are a high pass filter or neural networks [13,14,15]. A high pass filter generates a running average of the signal from each detector element in order to smooth out noise fluctuations. With a neural network, local neighbourhood sums are compared to pixel outputs in order to compute non-uniformities. Experiments have shown that these techniques can provide better sensitivity and thereby increase the operating dynamic range. Neural networks also offer the possibility of considerable image processing in the focal plane; for example, implementation of target recognition algorithms. Recent neural network developments include the silicon retina [61] in which some of the processing capabilities of the eye - background subtraction, edge enhancement and movement detection - have been implemented for optical wavelengths. Extension to IR wavelengths could be achieved by incorporating IR detectors.

With narrow gap semiconductors such processing is difficult to implement, necessitating the mating of the detector array to the processing electronics which is fabricated in a different material, typically silicon or possibly GaAs. However, a number of techniques are feasible including:

(a) Epitaxial growth of the detector on top of the processing electronics.

This is possible in MBE systems where lattice matched or graded buffer layers are grown between a substrate and detector material. Problems still occur in delamination of layers caused by stress build up, thus limiting the physical size. Multiple Quantum Wells (MQW) in GaAs are an exception where the detector and electronics can be the same material. Such detectors, however, require very low operating temperatures. Figure 7(c) shows a wire bonded architecture suitable for linear arrays. Front sided illumination for wire bonded linear arrays increases the available semiconductor processing area. 2D arrays are also possible with the loophole structure shown in Figure 7(e). In this arrangement a detector layer is bonded onto the readout electronics. A detector array is fabricated by ion-milling an array of holes, or interconnects, through to the underlying electronics. The ion-milling produces the detector diode by ion implantation, metallisation being needed to complete the circuit. The diodes thus formed are not

uniform and lead to some array uniformity problems. Secondly, it is also difficult to construct multiple layers for electronic non-equilibrium noise reduction schemes.

(b) Bonding of the detector array to the electronics.

With these hybrid technologies (Figure 7(a,b,d)), the detector array is bonded with indium contacts to the electronics. A 2D array of indium bumps, coincident with the detector elements, is deposited on the detector array. A second indium bump array of the same dimensions is deposited on the readout electronics, the two surfaces being mated together with temperature and physical pressure. The technique suffers from the mismatch of the different materials, limiting the array size and the available processing "real estate". Backside illumination (that is through the substrate which could be a microlens) is possible for these arrays. This has limitations on semiconductor "real estate" for signal processing (Figure 7(a)) but can be improved by using a fanout architecture (Figure 7(b)). A further technique which offers extensive processing area is the Z-technology where the detector is bonded to a stack of processing electronics. Limits occur due to material mismatch and to the thinning of the individual processors in the stack. The Z-technology is one approach used for neural networks as it provides considerable semiconductor real estate in a 3-dimensional structure which can facilitate the interconnects.

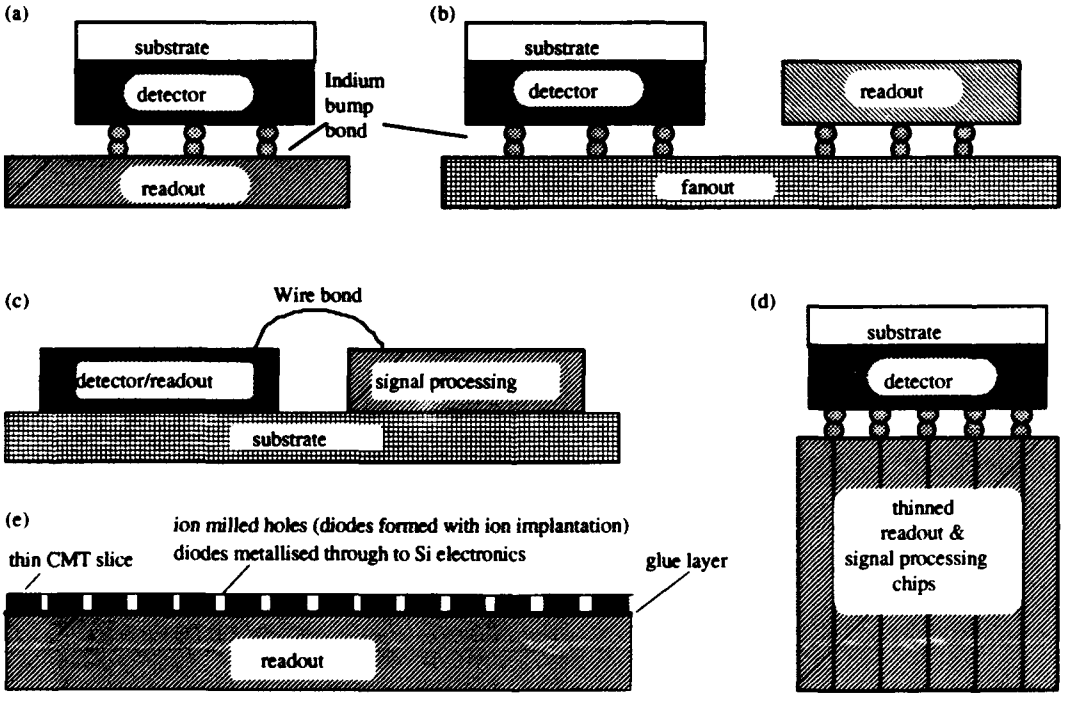

Figure 7. IR detector readout architectures: (a) direct hybrid, (b) indirect hybrid, (c) planar wire bonded, (d) Z technology, and (e) loophole.

4. MATERIALS CONSIDERATIONS

As stated earlier, high quality detector material will be a critical component in the next generation of photosensitive IR detector arrays. The materials in question in this report are: II-VI (CdHgTe), III-V (InSb & GaAs), IV-VI (Pb - chalcogenides) and some silicon based devices. These materials are narrow gap semiconductors with the exception of GaAs and Si. For the II-VI and IV-VI materials the band gap depends upon the composition, allowing the IR cut off wavelength to be tuned. InSb has a fixed gap with IR operation in the MWIR band only. Superlattices can, however, be made from alloys of this material (InSb/InAsSb) to allow LWIR operation. GaAs functions as an IR detector in the MWIR and LWIR bands when multiple quantum well structures are used.

4.1 II - VI (Cadmium Mercury Telluride)

Cadmium Mercury Telluride is an important semiconductor for IR detectors due to the band gap tailoring that can be achieved by suitable composition. This allows material to be made sensitive in the 3-5 μm and 8-12 μm bands or at other IR wavelengths between 1 and 25 μm. A number of materials exist which have similar MWIR performance but lesser material problems than CMT. The principal advantage of CMT is that detectors in the 8-12 μm band are available. This band is important in environments where dust and smoke obscure targets. Typically the transmission of LWIR is superior in these situations.

Photovoltaic (PV) detector diodes are preferred for large 2D arrays because of the low power consumption (hence less cooling needed), compared to photoconductive detectors which require biasing currents. From Table 1, it can be seen that PV CMT detectors need to be operated at low temperatures to reduce noise, although the techniques described earlier can be used to improve this for arrays. For example, Jones [8] et al bonded a microlens array on to a 128x1 CMT diode array and reported photocurrent gains of 10 to 12.

CMT does suffer formidable material problems [29] (nonuniformity, inhomogeneity, high defect density and impurities), although a considerable amount of work has gone into improving the crystal quality. A major problem is the level of mercury vacancies which results in p type material with a high background of carriers. This can be considerably reduced by annealing the epitaxial layer in a mercury vapour at 400-500°C. The purity of the Cd and Te source materials also needs to be improved so that the unintentional doping can be reduced. The reduction in mercury vacancies and unintentional doping is crucial to increasing the minority carrier lifetime for optimal device performance and for allowing the construction of multilayer structures which allow the operating temperature to be increased.

Stoichiometry is also very important as any deviations result in modification of the carrier concentration leading to poor spatial response uniformity. Consequently, detectors with low sensitivity but which are highly uniform, (for example, PtSi) can out perform the more sensitive CMT. There has been considerable research effort directed towards overcoming uniformity/homogeneity problems. A source of high compositional homogeneity CMT is from MBE, although this material still suffers from excess Hg

vacancies. LPE produces materials low in Hg vacancies due to the *in situ* mercury annealing that occurs during growth. However, this material has poor compositional homogeneity. *In situ* annealing with Hg vapour in the MBE chamber is very difficult. Post growth annealing may alter the introduced dopant concentrations and distribution, and consequently degrade the detector performance. Electronic means have been used for uniformity correction; that is, post detection amplification and offset which reduces the dynamic range of the system.

A number of 2D PV CMT arrays have been made, generally with backside (through the substrate) illumination. Front side illumination with wire bonding has been used for linear arrays. In the 3-5 μm band, operation at around 200K is possible while the 8-12 μm band requires cooling to 80K. Table 3 lists some of the arrays that are presently available in PV CMT. A large number of arrays with other formats have also been demonstrated [34] including; 32x1, 48x4 (TDI), 252x4 (TDI), 2x64 bi-spectral, 32x32 staring and 64x64 staring.

Table 3. Performance of some CMT arrays

Array	Ref	λ_c μm	T op K	D^* (300K) cm $Hz^{1/2}W^{-1}$	NEΔT K	Readout
288*4 TDI		10.3±0.1	77K	1.7×10^{11}		Direct CCD
240*4 TDI		$10.0 < \lambda < 10.5$	77K	$>1.2 \times 10^{11}$		
128*128 Staring	35	5.2±0.1	77K	3.2×10^{11}	12mK	Si CCD In bump bonded
128*128 Staring	35	3.2±0.1	200K	7×10^{11}	130mK	Si CCD In bump bonded
128*128 Staring	60	~4.5	180K	10^{11}	< 0.1K	CMOS
128*1 optically immersed	8	12.0	77K	1.9×10^{10} (500K)		measured photocurrent gain of 10
128*1 optically immersed	8	9.0	192K	1.7×10^{9} (500K)		measured photocurrent gain of 10
256*256 staring	27	4.9	80K	1.17×10^{12}	9mK	hybrid CMOS In bump bonded

TDI : Time delay integration. λ_c : cutoff wavelength

D^* : For 30° FOV and T_{bb} = 300K. NEΔT: Noise equivalent temperature difference of system.

The band gap tailoring also allows for the possibility of multi-band detection within the one detector by varying the composition. For example, a triple layer (n-p-n) heterojunction has been made with a hybrid MBE/LPE (Liquid Phase Epitaxy) growth technique [16]. The two back-to-back diode junctions (p/n) are of different composition and consequently of different cutoff wavelengths. By biasing the junctions

sequentially two colour detection is possible. A further technique is to use etching to produce side-by-side detectors but this has the disadvantage of a reduced fill factor and non-overlapping detectors.

Other mercury-based semiconductors — Mercury Zinc Telluride (MZT), Mercury Manganese Telluride (MMT) and Mercury Cadmium Manganese Telluride (MCMT) — are also promising materials [11,45,46] In particular, the dilute magnetic semiconductors (DMS), MMT and MCMT (manganese is a magnetic atom which leads to spin-spin exchange interactions between the localised magnetic moments and the band electrons) appear to offer some improvements in detector performance and fabrication compared to CMT. The materials have similar sensitivity and detectivity to CMT, they can be band gap engineered via composition changes for particular cutoff wavelengths and the R_oA product (see equation 1) appears to be superior. All of these factors should lead to better device performance. The DMS also have the possibility of magnetic tuning of the band gap due to the presence of manganese. The materials have crystal growth problems similar to CMT in terms of unintentional doping and mercury vacancies. However, it is thought that MZT and MMT would be more stable and that lattice matching to substrates is not as difficult as for CMT. Techniques similar to those employed for the growth of CMT are required for fabrication of detector arrays.

In summary, CMT and the other mercury-based semiconductors offer advantages for IR detector arrays at elevated temperatures. The flexibility of the material also allows multiple wavelength operation. The 8-12 μm band will probably be the wave band where CMT will find the greatest application. The main material problems appear to be the high intrinsic noise level primarily caused by Hg vacancies, material nonuniformity and the long term material stability. Annealing in Hg vapour has been shown to reduce the number of vacancies and the unintentional doping to low levels. *In situ* annealing (in the MBE chamber) appears difficult and other techniques may have to be found. Interfacing to readout electronics is a further problem which is limiting detector array areas to less than 1 cm^2. Epitaxial deposition on Si or GaAs substrates is hoped to overcome this problem. Multiple quantum wells (see next section) should also be possible once the problem of excess intrinsic noise is overcome. With the application of electronic non-equilibrium techniques and optical immersion, high temperature operation (~250K) appears possible for the 3-5 μm band. Higher temperature operation (> 80K) for the 8-12 μm band appears more difficult.

4.2 III - V (Indium Antimonide, Gallium Arsenide)

(a) Bulk material

A number of III-V materials have been used for IR detectors in a number of configurations. III-V materials have been used in hetero-structures, as strained layer superlattices and in multiple quantum wells. The primary III-V compound presently used in large arrays is Indium Antimonide (InSb) which has a cutoff wavelength of 5.5 μm. Indium Arsenide (InAs) with a cutoff of 3.5 μm has also been used but is obviously limited in use to the low end of the MWIR region. Both compounds require cooling to

around 80K and offer excellent performance. In general InSb is highly uniform and, combined with a well understood device fabrication and materials processing technology, leads to arrays with excellent spatial uniformity with quantum efficiencies greater than 50%. InSb also has smaller leakage currents than CMT across the diode junction and lower Auger recombination rates leading to lower noise levels. Large arrays up to 640 x 480 have been made for both high background operation or low background astronomy applications. Table 4 indicates some of the properties of typical arrays.

(b) Hetero-structures

Due to the intrinsic purity of InSb, electronic non-equilibrium noise reduction hetero-structures comprising InSb/$In_{1-x}Al_xSb$ layers (Figure 3) can be made [10]. As the temperature increases the 3 & 4 layer structures perform much better than the normal (2 layer) diodes. For example, the $p^+\pi n^+$ (3 layer) has to be cooled to 250K and the πn^+ to 180K to achieve the same performance as the $p^+p^+\pi n^+$ structure at room temperature. The high uniformity of these detectors is an advantage over other materials. However, their operation will still be limited to the MWIR band and two colour detectors cannot be made.

Room temperature $In_xGa_{1-x}As$ detector arrays for 2.5 μm (SWIR) have been made. These detectors are made by epitaxial deposition of graded hetero - structures on InP substrates [22]. Linear arrays with up to 256 elements with response between 1.7 and 2.5 μm and a quantum efficiency around 70% have been constructed. Their advantages over other material in this region (PbS, PbSe, CMT, InSb & InAs) are a continuously adjustable band gap and the lowest dark currents. CMT has a variable band gap but has materials problems at this wavelength.

Table 4. InSb type detectors.

Array	Ref	λ μm	T op K	D^* cm $Hz^{1/2}W^{-1}$	NEΔT K	Readout
InSb 128*128 Staring	19	1 - 5.5	80K	>4 x 10^{11}@80K >5 x 10^{12}@60K	10mK	
InSb 64*64 Staring	18	1 - 5.5	80K			Si Hybrid Bump bond
InSb 1*128	43	3 - 5	80K		40mK	Wire bond to Si multiplexer
InSb 1*128	17	3.3 - 5.5	60 - 120K	1.43 x 10^{11}		Wire bond to multiplexer
InSb 256*256	47	1.2 - 5.4	50K			Si multiplexed In bump bond
InSb 256*256	32	1 - 5.5	80K	>4 x 10^{11} @80K >5 x 10^{12} @ 60K	10mK	CMOS In bump bonded

(c) Strained Layer Superlattices

Superlattices have been proposed as an alternative device structure for IR detection. It is anticipated that superlattices would offer some advantages over "bulk" structures for IR detection. These include:

(i) higher degree of uniformity;

(ii) smaller leakage currents due to the suppression of tunnelling;

(iii) lower Auger recombination rates in some superlattices;

(iv) well understood device fabrication and materials processing technology.

These advantages have not been realised as yet due to the difficulty in making the superlattices. Initial efforts have been with HgTe/CdTe layers. Significant interest has now been shown in InSb/$InAs_{1-x}Sb_x$ and $Ga_{1-x}In_xSb$/InAs strained layer superlattices with band gaps corresponding to wavelengths greater than 10 μm reported and it has been estimated that 14 μm band gaps may be possible [20,21]. Strained layer superlattices (SLS) are made by epitaxial deposition of multiple (up to 50) alternate thin layers (2.5 -7 nm) of semiconductors with slightly different lattice parameters. The cutoff wavelength is determined by the material and the layer thickness. Spontaneous strained layers have been shown to form in InSb/$InAs_{1-x}Sb_x$ for mid-range x compositions which severely degrade the performance of the material. GaInAs/InAs, although highly strained, offer some advantages as the GaInAs layer can be lattice matched to GaAs substrates. Low background carrier concentrations (unintentional doping) are difficult to achieve in both materials and it is desirable to reduce these to as low a value as possible to minimise noise sources. Considerable work will be required to overcome the material problems and also low temperature operation will be required.

In summary, InSb detectors are well established in the MWIR band and operate at low (77K) temperatures. Their main advantages are high uniformity and mature fabrication technology. Non-equilibrium techniques can be used due to low intrinsic noise sources, and when combined with optical immersion, could lead to room temperature operation in the MWIR band. Extended operation to LWIR is possible with SLS, although some materials problems exist. Electronic non-equilibrium techniques are only applicable to "bulk" material and cannot be applied to SLS (or multiple quantum wells).

(d) Multiple Quantum Wells

The developments of superlattice structures has provided possibilities for extending other III-V materials into the far IR by construction of multiple quantum wells. A quantum well is formed by depositing a thin (3-5 nm) semiconductor layer between two thicker (10-50 nm) barrier layers. This produces confined states within the quantum wells of the semiconductor. Structures with IR absorption between a bound state and the continuum can be constructed. A multiple quantum well is made by depositing a number of layers, as shown schematically in Figure 8.

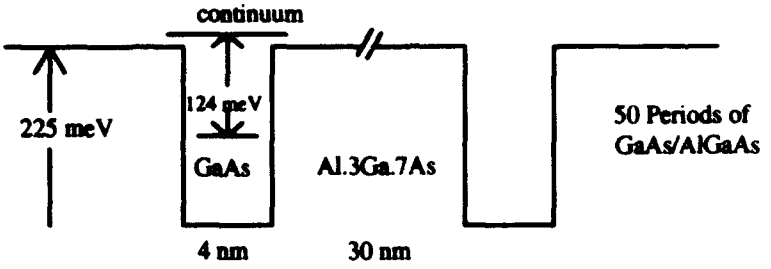

Figure 8. GaAs/AlGaAs MQW designed for maximum 10 μm operation.

The peak absorption wavelength is dependent upon the material and the layer thickness. Table 5 gives an indication of the absorption peak as a function of barrier thickness for a GaAs MQW. The optical transition is between a bound state and the continuum. This results in an absorption width of the order of 1-2 μm. The 50 nm sample was characterised by maximum detectivity of $4x10^{13}$cm $Hz^{1/2}W^{-1}$ @ 6K and was essentially constant to 50K before falling rapidly to $2x10^{10}$cm $Hz^{1/2}W^{-1}$ @ 80K [23]. This high sensitivity is sufficient for most imaging applications, pixel non-uniformity being the limiting factor. It has also been shown [40] that photoconductive gain in QW infrared photodetectors is possible for particular designs. This should lead to improved detectivity.

Table 5. Peak absorption vs barrier thickness (well thickness 4μm)

Barrier thickness	30 nm	40 nm	50 nm
peak absorption μm	7.5	8.3	8.5

GaAs MQWs can be made to operate in the 3-5 μm band and up to 15 μm. D^* for the extended wavelength operation was found to be 10^9cm $Hz^{1/2}W^{-1}$ at 77K and increased to 10^{12}cm $Hz^{1/2}W^{-1}$ at 33K [26]. In a further development, a GaAs/AlGaAs quantum well detector with a voltage tunable spectral sensitivity at 3-5 and 8-12μm has been reported [33]. The relative intensity of the photo response in these two bands depends strongly on the bias voltage, demonstrating the potential for such a structure to function as a two colour detector.

The potential advantages of GaAs MQWs include:

(i) standard manufacturing processes,

(ii) high uniformity, high yield and well controlled MBE growth,

(iii) monolithic integration into GaAs signal processing electronics,

(iv) multi-spectral detection.

Excessive dark currents generated by thermionic emission at higher temperatures are a major problem which lead to large non-uniformities in the detectivity of elements even though GaAs material is quite uniform and impurity free [24]. Linear scanned arrays (10 elements) [30] with NEΔT of <0.1K and 2D arrays up to 128*128 operating at temperatures less than 80K (Table 6) have been reported.

A further problem with multiple quantum wells is coupling the light into the detector. Selection rules dictate that only photons with a component of electric field normal to the quantum well can excite

Table 6. GaAs MQW type detectors.

Array	Ref	λ μm	T op K	D^* cm $Hz^{1/2}W^{-1}$	NEΔT K	Readout
10*1	30	9	<80K	8×10^9 @ 77K 1×10^{13} @ 36K	<0.1	
128*128	31	7.9	77K	3.1×10^{10}	<10mK	
128*128	28	7.7	<80K	5.76×10^9 @80K	30mK	In bump bonded. CMOS.
128*128	26	9	60K		10mK	In bump bonded. Si multiplexer

transitions in *n*-type QWs and can therefore be absorbed. Typical detector geometries, where the IR signal is normal to the surface, would have zero absorption for MQWs. Gratings or bevelled edges [36,37] have been developed to couple the IR radiation to the detector (Figure 9). Bevelled edges, which are only applicable to linear arrays have low optical coupling efficiency, (typically 0.2), caused by inherent losses in the technique. Sawtooth gratings etched onto the substrate allow normal incidence with the grating coupling light into the detectors quite efficiently (up to 90% grating efficiency). In *p*- type QWs [38] all polarisation's are allowed which makes them more favoured for normal incidence detectors. A long wavelength, 7.9μm peak detection has been demonstrated in a *p*- type GaAs quantum well with a $D^*$of 3.1×10^{10} cm $Hz^{1/2}W^{-1}$ at 77°K [31,39]. This diode had a normal incidence quantum efficiency of 28%. Indirect gap semiconductors (AlAs/AlGaAs) have also been made into MQWs. Such materials show strong normal absorption between 5 and 20 μm and may form excellent IR detectors [48].

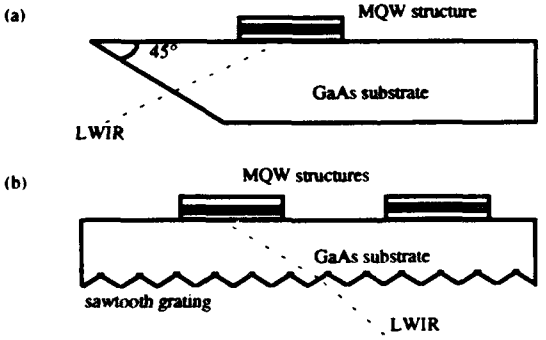

Figure 9. Schematic MQW optical coupling schemes. (a) bevel edge (b) sawtooth grating.

In summary, GaAs/AlGaAs multiple quantum wells have demonstrated good sensitivity for PC detectors with LWIR peak detection at low temperatures. Further improvements are expected. Two colour operation also appears possible by simple biasing of the quantum well. Excessive dark currents are a problem and require operating temperatures to be less than 80K. The advantages are, well understood GaAs technology, ability to produce uniform material, and compatibility with Si technology. Tailored band gap profiles are also possible with atomic control over layer thickness enabling selected infrared detection from 3 to 15 μm.

4.3 IV - VI (Lead Chalcogenides)

Lead salts (PbS & PbSe) were the first practical direct gap IR detector materials. Linear arrays were fabricated in the 1960s shortly after photolithography was developed. These were slow photoconductive devices. In the 1970s PC CMT arrays were developed, having faster response times, thus allowing the development of linear scanning arrays. Because of this, work on lead salts ceased. The properties of lead salts which caused problems when compared to CMT in the 1970s were [41,42]:

(i) high permittivity of IV-VIs make them too slow when used in scanning systems;

(ii) PC detectors were preferred to interface to electronics whereas, single crystal IV-VI were suitable for PV use due to their high carrier concentration;

(iii) IV-VIs are soft, difficult to handle and have a high thermal expansion coefficient:

(iv) they are less flexible in their use since different materials are required to cover the different wavelengths required (Table 7).

Table 7. Cutoff wavelength for IV-VI materials.

Detector	Cutoff wavelength μm.
PbS	3.0 (300K) 4.0 (77)
PbSe	4.6 (300K) 7.0 (77K)
PbTe	4.0 (300K) 5.6 (77K)
$PbS_{1-x}Se_x$ (x = 0-1)	3 - 7
$Pb_{1-x}Eu_xSe$ (x = 0-≈0.02)	7 - 3
$Pb_{1-x}Sn_xSe$ (x = 0-≈0.2)	7 - ∞ (77K)
$Pb_{1-x}Sn_xTe$ (x = 0-≈0.4)	4 - ∞ (77K)

For PC detectors these problems were considerable in the 1970's, the period when first generation CMT detectors were developed. However, two dimensional PV staring arrays are now preferred and the perceived problems no longer exist. The speed of the IV-VI material for staring arrays is satisfactory and the higher permittivity means greater storage and hence greater dynamic range on the detector array. The higher permittivity also allows a higher carrier concentration compared to CMT. This is more controllable and the residual impurity level can be higher. The softness is not a problem once the arrays are deposited on Si substrates and actually helps to overcome the thermal expansion problem by allowing some stress reduction. Other advantages compared to CMT for staring arrays include:

(a) Material technology is easier and there is no material stability or diffusion (Hg) problem. High composition uniformity is also achievable and the cutoff wavelength is less sensitive to the composition of the semiconductor.

(b) The higher permittivity effectively shields the electric fields of charged defects making the material fault tolerant. High performance sensors can be made from material with a high density of lattice defects.

(c) The optical absorption is higher and detectors can be made from thinner layers.

The detectors are MBE grown on Si substrates with stacks of CaF_2 - BaF_2 bilayers for lattice matching. These layers also help to overcome the thermal expansion mismatch between the substrate and detector material. Linear sensor arrays of 66 and 256 elements [41,42] have been made with standard Al metallisation. A 256*1 array [44] has also been made by the deposition of PbSe on a single crystal quartz substrate. This was then wire bonded to a standard Si CMOS multiplexer. Table 8 gives the performance parameters for these arrays.

Table 8. Lead chalcogenide type detectors.

Array	λ μm	T op K	D^* cm $Hz^{1/2}W^{-1}$	NEΔT K	Readout
66*1 $Pb_{1-x}Sn_xSe$ (& 256*1)	10.5	77	8×10^{10} @ 77°K		Si VLSI integrated
256*1 PbSe [44]	5.3	190	3.35×10^{10}	0.2	Wire bonded CMOS

In summary, arrays have been fabricated in PbTe, PbSe, $Pb_{1-x}Sn_xSe$, PbS, $Pb_{1-x}Eu_xSe$ and $PbS_{1-x}Se_x$ with cutoff wavelengths between 3 and 12 μm. At present IV-VI IR detectors are inferior compared to CMT but it is believed [42] that improved fabrication processes will increase the performance. Advantages are compatibility with Si VLSI processing, material homogeneity and that only thin layers are required. Elevated operating temperatures are also believed to be possible. The main disadvantages centre on the need for different materials to make MWIR and LWIR detectors. This lack of flexibility makes fabrication of two colour detectors more difficult.

4.4 IV (Si based photo detectors)

Although silicon technology is mature, recent developments have shown that some further improvement is possible. Silicon based materials have generally been used for visible and near IR (<1.25 μm) detector arrays due to the IR cutoff wavelength in silicon. Extrinsic Si, however, has a VLWIR cutoff when cooled to 4K and has been used as a detector at these wavelengths. Platinum silicide (PtSi) was developed as an IR detector and, using back side illumination, is characterised by a cutoff wavelength of around 5.5 μm. IrSi (Iridium silicide) can be used at slightly longer wavelengths. Low temperature operation (77K) is required to reduce the dark current. These arrays generally have a very low quantum efficiency (~0.1% at 5 μm) but their high material homogeneity and pixel uniformity results in detectors that out-perform more sensitive material [4]. By incorporating an optical cavity in the PtSi detector structure, the quantum efficiency at lower wavelengths (2 -3 μm) can be raised. Efficiencies approaching 10% have been obtained [55] at these wavelengths. Infrared cameras, using large PtSi arrays (512*512. 640*480), are currently in production and are available [64]. Visible and ultra-violet (UV) detection [49] is also possible with these materials using front-side illumination. A four band 4096 element linear detector integrated onto a single substrate utilising PtSi has been developed for remote sensing

applications [50]. The device is operated at 77K with bands centred on 1.655 μm, 2.065 μm, 2.190 μm and 2.335 μm.

Recently there have been further developments in Si based detectors to extend the cutoff wavelength into the LWIR band. These new detectors are heterojunctions [51], strained layer superlattices [52] and a simple homo-junction [53] structure. The hetero-structure is based on SiGe/Si and is characterised by a quantum efficiency of around 1% (when operated at 77K) and a wavelength cutoff greater than 12 μm. At lower temperatures the quantum efficiency reaches 3-4 % which is much greater than the "bulk" PtSi or IrSi detectors. A strained layer superlattice based on Ge_xSi_{1-x}/Si shows an IR response out to 14 μm when operated at low temperatures (<77K). The silicon homo-junction is a thin insulating layer placed between two conductive layers. With this structure a potential barrier to electronic conduction is formed between the two conductive layers. Absorption of infrared radiation by charge carriers, (for example, electrons) can give the carriers enough energy to overcome the barrier. The detected current is a measure of the infrared flux incident onto the junction. The height of the potential barrier can be varied by changing the layer thickness and doping. Cutoff wavelengths out to 13 μm have been demonstrated at low temperatures (50K). These three techniques will only work at low temperatures as the noise increases dramatically with temperature. A room temperature Si based IR detector has also been demonstrated [54]. The detector is based on the thermal properties of the Si diode junction and is a two stage thermal detector. A separate absorbing layer is deposited on top of the junction to improve the IR absorption. The sensitivity was not very high ($D^* = 6 \times 10^5 cm\ Hz^{1/2}W^{-1}$). However, it was hoped that with further development it would improve.

In summary, the great advantage of using Si based detectors is the mature silicon IC technology. These systems may provide a high sensitivity, high uniformity, long wavelength IR detector and lead to very large scale focal plane arrays in the 8 - 12 μm range. Low temperature operation will be necessary. PtSi is a mature technology. The high uniformity of PtSi results in large high performance MWIR arrays that out-perform more sensitive but less uniform material.

5. CONCLUSIONS

The choice of material for an IR detector is not straightforward and to a large degree depends upon the required wavelength, the type of application and the desired operating temperature. The probable requirements for the next generation of infrared photon sensor can be summarised as follows:

(a) large format staring array (10^4 - 10^6 elements) operating at TV frame rates,

(b) large linear arrays (480*4 up to 4096*4) for wide angle viewing.

(c) multi-spectral (3-5, 8-12 μm) and multi band (UV - IR, IR - mm-wave) operation to increase detection probability, reduce false alarm rates and perform automatic target detection/recognition.

(d) focal plane processing for real time image analysis/identification.

(e) near room temperature operation,

(f) capability for multi-sensor device fusion.

Considering these requirements a number of points can be made in regard to the materials discussed:

(1) In the MWIR and LWIR band MQWs and strained layer superlattices have advantages at low temperatures (<80K), mainly due to the high uniformity possible with GaAs. Also in the MWIR band PtSi and InSb, both operating at 77K, have advantages due to their high uniformity. It has been shown that pixel uniformity and not detectivity limits imaging quality with these materials. The mature technology and electronic processing available with Si and GaAs is an advantage.

(2) CMT has advantages in LWIR operation. Material problems such as the intrinsic noise still need to be solved and bonding of large arrays to Si readouts is difficult.

(3) For near room temperature operation in the MWIR band with narrow gap semiconductors, electronic non equilibrium and optical immersion techniques will be required. InSb has the purity and uniformity requirements for these two techniques. InSb/InAlSb hetero-structures with optical immersion may also be used for the MWIR band near room temperature due to its high uniformity and mature materials technology. Multi-spectral operation (LWIR) is not possible. Considerable improvements in the growth of CMT will be needed to employ non-equilibrium techniques. LWIR operation at near room temperature appears to be very difficult with current semiconductors.

(4) Other materials, (eg DMS, CdZnTe and the Pb-chalcogenides) are interesting but their present development is limited. The Pb-chalcogenides are very interesting for array applications and may have advantages over CMT in the LWIR band. Their future development should be monitored to assess where the technology is leading.

In conclusion, advances in IR detector technology are occurring in materials improvements and in signal processing. The materials improvements: non-equilibrium structures, micro-lenses, multiple quantum wells, superlattices, are leading to higher temperature operation and the development of dual band detectors. These improvements can be considered incremental in many cases and are providing improved sensor operation. Major advances leading to significant (x10 - 100) improvements in detection or noise levels are more difficult. Significant advances in signal processing can also be expected.

REFERENCES

1	R. Balcerak	Infrared material requirements for the next generation of systems. Semiconductor Science Technology **6** (1991) pp C1-C5.
2	D.A. Scribner, M.R. Kruer & J.M. Killiany.	Infrared Focal Plane Array Technology. Proc of the IEEE. Vol 79 1991 pp 66-85.
3	P.R. Norton.	Infrared image sensors. Optical Engineering. V30 #11 1991 pp1649-1663.
4	P.R. Norton & W. Radford.	Responsivity uniformity of infrared detector arrays. Semicond. Sci. and Technol. **6** 1991 pp C96-C98.
5	N.T. Gordon, C.L. Jones & D.J. Purdy.	Application of Microlenses to Infrared Detector Arrays. Infrared Physics V31 #6 1991 pp 599-604.
6	N.T. Gordon.	Design of $Hg_{1-x}Cd_xTe$ infrared ... ctor arrays using optical immersion with microlenses to achieve a higher operating temperature. Semicond. Sci. Technol. **6** 1991 pp C106-C109.
7	T. Werner, J.A. Cox, S. Swanson & M. Holz.	Microlens array for staring infrared imager. SPIE Vol 1544 Minature and Micro -Optics. Fabrication and System Applications. 1991 pp 46-57.
8	C.L. Jones, B.E. Mathews, D.R. Purdey & N.E. Metcalfe	Fabrication and assessment of optically immersed CdHgTe detector arrays. Semicond. Sci. Technol. **6** 1991 pp C110-C113.
9	M.E. Motamedi, W.H. Southwell, R.J. Anderson, L.G. Hale & W.J. Gunning.	High speed binary optic microlens array in GaAs. SPIE Vol 1544 Minature and Micro -Optics. Fabrication and System Applications. 1991 pp 33-44.
10	T. Ashley & C.T. Elliott.	Operation and properties of narrow-gap semiconductor devices near room temperature using non-equilibrium techniques. Semicond. Sci. Technol. **6** 1991 pp C99-C105.
11	J. Piotrowski.	Recent advances in IR Detector Technology. Microelectronics Journal. 23 (1992) pp 305-313.
12	D.A. Scribner, K.A. Sarkady, M.R. Kruer, J.T. Caulfield, J.D. Hunt & C. Herman.	Adaptive non uniformity correction for IR focal plane arrays using neural networks. SPIE V 1541 Infrared Sensors: Detectors, Electronics, and Signal Processing 1991 pp100-109.
13	J.C. Carson	On-focal plane array feature extraction using a 3D artificial neural network (3DANN^{TM}) Part I. SPIE V 1541 Infrared Sensors: Detectors, Electronics, and Signal Processing 1991 pp 141-144.
14	J.C. Carson.	On-focal plane array feature extraction using a 3D artificial neural network (3DANN^{TM}) Part II. SPIE V 1541 Infrared Sensors: Detectors, Electronics, and Signal Processing 1991 pp 227-231.

15	T.S. Jayadev.	Focal plane architectures and signal processing. SPIE V 1541 Infrared Sensors: Detectors, Electronics, and Signal Processing 1991 pp 163-166.
16	O.K. Wu & G.S. Kamath.	An overview of HgCdTe MBE technology. Semicond. Sci. Technol. 6 1991 pp C6-C9.
17	J.J. Forsthoefel, R.M. Davis, C.A. Niblack & J.E. Doles.	Performance of a linear multiplexed MWIR FPA featureing buffered direct injection. SPIE V 1157 Infrared Technology XV 1989 pp 115-121.
18	C.A. Niblack, H.A. Timlin, C.J. Martin, R.C. Fisher, C. Walmsley & C. Steel.	Initial characterization of a new 64x64 mutiplexed InSb FPA. SPIE V 1157 Infrared Technology XV 1989 pp 124-132.
19	J. Blackwell, S Botts, A. Laband & H. Arnold.	An affordable 128 x 128 InSb hybrid focal plane array. SPIE V 1157 Infrared Technology XV 1989 pp 243-249.
20	R.A. Stradling.	InSb-based materials for detectors. Semicond. Sci. Technol. 6 1991 pp C52-C58.
21	D.H. Chow, R.H. Miles, J.N. Schulman, D.A. Collins & T.C. McGill.	Type II superlattices for infrared detectors and devices. Semicond. Sci. Technol. 6 1991 pp C47-C51.
22	G.H. Olsen, A.M. Joshi, S.M. Mason, K.M. Woodruff, E. Mykietyn, V.S. Ban, M.J. Lange, J. Hladky, G.C. Erickson & G.A. Gasparin.	Room-temperature InGaAs detector arrays for 2.5 μm. SPIE V 1157 Infrared Technology XV 1989 pp 276-282.
23	W Bloss, M. O'Loughlin & M. Rosenbluth.	Advances in Multiple Quantum Weii IR Detectors. SPIE V 1541 Infrared Sensors: Detectors, Electronics, and Signal Processing 1991 pp 2-10.
24	F.W. Adams, K.F. Cuff, G. Gal, A. Harwit & R.L. Whitney.	A critical look at AlGaAs/GaAs multiple-quantum-well infrared detectors for thermal imaging applications. SPIE V 1541 Infrared Sensors: Detectors, Electronics, and Signal Processing 1991 pp 24-37.
25	S.D. Gunapala, B.F. Levine, D. Ritter, R. Hamm & M.B. Panish.	InP based quantum well infrared photodetectors. SPIE V 1541 Infrared Sensors: Detectors, Electronics, and Signal Processing 1991 pp 11-23.
26	B.F. Levine, G.C. Bethea, K.G. Glogovsky, J.W. Stayt & R.E. Leibenguth.	Long-wavelength 128 x 128 GaAS quantum well infrared photodetector arrays. Semicond. Sci. Technol. 6 1991 pp C114-C119.

27	R.B. Bailey, L.J. Kozlowski, J. Chen, D.Q. Bui, Kadri Vural, D.D. Edwall, R.V. Gil, A.B. Vanderwyck, E.R. Gertner & M.B. Gubala.	256 X 256 Hybrid HgCdTe Infrared Focal Plane Arrays. IEEE Transactions on Electron Devices. V 38 #5 1991 pp 1104-1109.
28	L.J. Kozlowski, G.M. Williams, G.J. Sullivan, C.W. Farley, R.J. Anderson, J. Chen, D.T. Cheung, W.E. Tennant & R.E. DeWames.	LWIR 128 x 128 GaAs/AlGaAs Multiple Quantum Well Hybrid Focal Plane Array. IEEE Transactions on Electron Devices. V 38 #5 1991 pp 1124-1130.
29	A. Sher, M.A. Berding, M. van Schilfgaarde & An-Ban Chen.	HgCdTe status review with emphasis on correlations, native defects and difusion. Semicond. Sci. Technol. 6 1991 pp C59-C70.
30	C.G. Bethea, B.F. Levine, V.O. Shen, R.R. Abbott, & S.J. Hseih.	10 μm GaAs / AlGaAs Multiquantum Well Scanned Array Infrared Imaging Camera. IEEE Transactions on Electron Devices. V 38 #5 1991 pp 1118-1123.
31	B.F. Levine, G.C. Bethea, J.W. Stayt, K.G. Glogovsky, R.E. Leibenguth, S.D. Gunapala, S.S. Pei & J.M. Kuo.	Long wavelength GaAs/$Al_xGa_{1-x}As$ quantum well infrared photodetectors (QWIPs). SPIE V 1540 Infrared Technology XVII 1991 pp 232 - 237.
32	J.D. Blackwell, W.J. Parrish & G.T. Kincaid.	High performance InSb 256 x 256 Infrared camera. SPIE V 1479 Surveillance Technologies 1991 pp324 - 334.
33	K. Kheng, M. Ramsteiner, H. Schneider, J.D. Ralston, F. Fuchs & P. Koidl	Two-colour GaAs/(AlGa)As quantum well infrared detector with voltage-tunable spectral sensitivity at 3-5 and 8-12 μm. Appl. Phys. Lett. 61 (6) 1992 pp 666-668.
34	J.P. Chatard.	SOFRADIR IR focal plane array production. SPIE V 1341 Infrared Technology XVI 1990 pp316-323
35	E. Mottin, J.P. Chamonal, D. Marion, F. Mongellaz, P. Nicolas & J.L. Tissot.	128 x 128 3-5 μm focal plane arrays at 77K and 200K operation. SPIE V 1341 Infrared Technology XVI 1990 pp 375-383
36	G. Hasnain, B.F. Levine, C.G. Bethea, R.A. Logan, J. Walker & R.J. Malik.	GaAs/AlGaAs mulitquantum well infrared detector arrays using etched gratings. Appl. Phys. Lett. V 54 (25) 1989 pp2515-2517.
37	K.W. Goossen, S.A. Lyon & K. Alavi.	Grating enhancement of quantum well detector response. Appl. Phys. Lett. V 53 (12) 1988 pp1027-1029.
38	H.H. Chen, M.P. Houng & Y.H. Wang.	Normal incidence intersubband optical transition in GaSb/InAs superlattices. Appl. Phys. Lett. V 61 (5) 1992 pp509-511.
39	B.F. Levine, S.D. Gunapala, J.M. Kuo, S.S. Pei & S. Hui.	Normal incidence hole intersubband absorption long wavelength GaAs/$Al_xGa_{1-x}As$ quantum well infrared photodetectors. Appl. Phys. Lett. V 59 (15) 1991 pp1864-1866.

40	G. Hasnain, B.F. Levine, S. Gunapala & Naresh Chand.	Large photoconductive gain in quantum well infrared photodetectors. Appl. Phys. Lett. V 57 (6) 1990 pp608-610.
41	H. Zogg, C. Maissen, J. Masek, T. Hoshino, S. Blunier & A.N. Tiwari.	Photovoltaic infrared sensor arrays in monolithic lead chalcogenided on silicon. Semicond. Sci. Technol. 6 1991 pp C36-C41.
42	H. Zogg, S. Blunier, T. Hoshino, C. Maissen, J. Masek, & A.N. Tiwari.	Infrared sensor arrays with 3-12 μm cutoff wavelengths in heteroepitaxial narrow-gap semiconductors on silicon substrates. IEEE Transactions on Electron Devices. V 38 #5 1991 pp 1110-1117.
43	H. Fujisada, M. Nakayamu & A. Tanaka.	Compact 128 InSb focal plane assembly for Thermal Imaging. SPIE V 1341 Infrared Technology XVI 1990 pp 80-91.
44	J.F. Kreider, M.K. Preis, P.C.T. Roberts, L.D. Owen , W.M. Scott, C.F. Wamsley & A. Quin.	Multiplexed mid-wavelength IR long, linear photoconductive focal plane arrays. SPIE V 1488 Infrared Imaging System Design, Analysis, Modeling and Testing II. 1991 pp 376-388.
45	J.M. Pawlikowski.	Diluted magnetic semiconductors based on II-VI compounds for photovoltaic detector applications. Infrared Physics V30 pp 295-305 1990.
46	J. Piotrowski, W. Galus & M. Grudzin.	Near room-temperature IR photo-detectors. Infrared Physics V31 pp 1-48 1991.
47	A Hoffman & D. Randall.	High performance 256 x 256 InSb FPA for Astronomy. SPIE V 1540 Infrared Technology XVII 1991 pp 297 - 302.
48	J. Katz, Y. Zhang & W.I. Wang.	Normal incidence infrared absorption in AlAs/AlGaAs x-valley multiquantum wells. Appl Phys Lett 61 (14) 1992 pp 1697 - 1699.
49	C.K. Chen, B. Nechay & Bor-Yeu Tsaur.	Ultraviolet, Visible, and Infrared Response of PtSi Schottky-Barrier Detectors Operated in the Front -Illuminated Mode. IEEE Trans on Electron Devices. Vol 38 #5 1991 pp 1094 - 1103.
50	M. Denda, M. Kimata, S. Iwade, N. Yutani, T. Kondo & N. Toubouchi.	4 Band x 4096-Element Schottky-barrier Infrared linear Image sensor. IEEE Trans on Electron Devices. Vol 38 #5 1991 pp 1131 - 1135.
51	True-Lon Lin, A. Ksendzov, S.M. Dejewski, E.W. Jones, R.W. Fathauer, T.N. Krabach & J. Maserjian.	SiGe/Si hetrojunction internal photoemission long-wavelength infrared detectors fabricated by molecular beam epitaxy. IEEE Trans on Electron Devices. Vol 38 #5 1991 pp 1141 - 1144.
52	R. People, J.C. Bean, C.G. Bethea, S.K. Sputz & L.J. Peticolas.	Broardband (8 - 14 μm), normal incidence, pseudomorphic Ge_xSi_{1-x}/Si strained layer infrared photodetector operating between 20 and 77K. Applied Physics Letters 61 (9) 1992 pp1122 - 1124.
53	S. Tohyama, N. Teranishi, K. Konuma, M. Nishimura, K. Arai & E. Oda.	A new concept Silicon homojunction infrared sensor. IEEE Trans on Electron Devices. Vol 38 #5 1991 pp 1136 - 1140

54	A. Tanaka, M. Suzuki, R. Asahi, O. Tabata & S. Sugiyama.	Infrared linear image sensor using a poly - Si pn junction diode array. Infrared Physics 33 (4) 1992 pp 229 - 236.
55	W.F. Kosonocky & G.W. Hughes.	High fill factor Silicide monolithic arrays. SPIE v782. Infrared Sensors and Sensor Fusion. 1987 pp 114 - 120
56	R.E. Flannery & J.E. Miller.	Status of uncooled infrared imagers. SPIE V 1689 Infrared Imaging Systems. (1992) pp 379 - 395.
57	K.C. Liddiard.	Thin film monolithic detector arrays for uncooled thermal imaging. SPIE V 1969 Optoelectronic engineering/ aerospace (Orlando 1993)
58	O.M. Williams.	A critique on the application of infrared photodetector theory. Infrared Physics #3 V 26 1986 pp 141 - 153
59	M.B. Stern, W.F. Delaney, M Holz, K.P. Kunz, K.R. Maschhoff & J. Welsch.	Binary optic microlens arrays in CdTe. Materials Research Society. Symp. Proc. V216 1991 pp 107 - 112.
60	L.J. Kozlowski, S.L. Johnston, W.V. McLevige, A.H.B. Vanderwyck, D.E. Cooper, S.A. cabelli, E.R. Blazejewski, V. Vural & W.E. Tennant	128*128 PACE I HgCdTe hybrid FPAs for thermoelectrically cooled applications. SPIE V 1685 Infrared Detectors and Focal Plane Arrays II 1992 pp 193 - 404
61	M.A. Mahowald & C. Mead	The Silicon Retina. Scientific Americian. May 1991 pp 40 - 46
62	Z. Djuric & J. Piotrowski	Room temperature IR photodetector with electromagnetic carrier depletion. Electronics Letters. V26 pp 1689 - 1691 1990
63	Z. Djuric, V. Jovic, M. Matic & Z. Jaksic	IR photodetector with exclusion effect and self filtering n^+ layer. Electronic Letters. V26 pp929 - 931. 1990
64	J.R. Tower	PtSi thermal imaging systems: A new level of performance and maturity. Photonics Spectra. April 1991. (David Sarnoff Research Center. Thermal Imager)

THIS IS A BLANK PAGE

DISTRIBUTION LIST

Defence Science and Technology Organisation

Chief Defence Scientist Central Office Executive	} 1 shared copy with CDS
Counsellor, Defence Science London	Control Sheet
Counsellor, Defence Science Washington	Control Sheet
Senior Defence Science Advisor	1 copy
Director, ASSA	1 copy
Scientific Advisor, Navy	1 copy
Scientific Advisor, Air Force	1 copy
Scientific Advisor, Army	1 copy
Scientific Advisor, Polcom	1 copy

Surveillance Research Laboratory, DSTO

Director	1 copy
Chief, Land, Space and Optoelectronics Division	1 copy
Research Leader, Optoelectronics Sensors & Systems	1 copy
Head, Smart Sensors (K Liddiard)	1 copy
P.J. Picone	2 copies

Libraries and Information Services

OIC, Technical Reports Central Library Campbell Park	1 copy
Manager, Document Exchange Centre, Defence Information Services	1 copy
Defence Research Information Centre, United Kingdom	2 copies
National Tehnical Information Service, United States	2 copies
Director Scientific Information Services, Canada	1 copy
Ministry of Defence, New Zealand	1 copy
National Library of Australia	1 copy
Defence Science and Technology Organisation Salisbury, Research Library	2 copies
MRL Maribyrong Library	1 copy
ARL Fisherman's Bend, Library	1 copy
Library DSD	1 copy
AGPS	1 copy
British Library. Document Supply Centre	1 copy

Spares

Defence Science and Technology Organisation Salisbury. Research Library	6 copies

THIS IS A BLANK PAGE

Department of Defence
DOCUMENT CONTROL DATA SHEET

Page Classification
UNCLASSIFIED
Privacy Marking/Caveat (of Document) N/A

1a. AR Number	1b. Establishment Number	2. Document Date	3. Task Number
AR - 008 - 157	SRL - 0117 - RR	December 93	DST 92/454

4. Title	5. Security Classification
ADVANCED INFRARED PHOTODETECTORS (MATERIALS REVIEW)	6. No of Pages 28 7. No of refs 64 U/C Document U/C Title U/C Abstract S (Secret) C (Confi) R (Rest) U (Unclass) * For UNCLASSIFIED docs with a secondary distribution LIMITATION, use (L) in document box.
8. Author(s) Philip J. Picone.	9. Downgrading/Deliminting instructions N/A
10a. Corporate Author and Address Surveillance Research Laboratory PO Box 1500 Salisbury SA 5108 10b. Task Sponsor	11. Officer/Position responsible for Security.....N/A..... Downgrading.....N/A..... Approval for Release.....DSRL.....

12. Secondary Distribution of this Document

APPROVED FOR PUBLIC RELEASE

Any enquires outside stated liminations should be referred through DSTIC, Defence Information Services, Department of Defence, Anzac Park West, Canberra, ACT 2600

13a. Deliberate Announcement

No Limitation

13b. Casual Announcement (for citation in other documents)

No Limitations
Ref. by Author, Doc No. and date only

14. DEFTEST Descriptors	15. DISCAT Subject Codes
Infrared Detectors, Materials, Photodetectors, Semiconductors (materials)	170501 , 11

16. Abstract

The present status of advanced infrared semiconductor detector materials and their application to infrared sensor array systems is reviewed. Techniques to increase device operating temperature are considered for various materials. Focal plane processing requirements are also considered.